Mathematical Modelling Of Nanoscale Phenomena

T. G. Myers, F. Font, M. M. MacDevette

Centre de Recerca Matemàtica, Barcelona, Spain

ABSTRACT

This paper concerns a selection of nanoscale problems currently being investigated, using continuum theory, by the research group at the CRM:
1. Enhanced flow in carbon nanotubes (CNTs) – This model shows that the experimentally observed enhancement can be explained using standard flow equations but with a depletion layer between the liquid and solid interfaces.
2. Nanoparticle melting – Nanoparticles often exhibit a sharp increase in melting rate as the size decreases. A mathematical model will be presented which predicts this phenomena.
3. Nanofluids – Experimental results concerning the remarkable heat transfer characteristics of nanofluids are at times contradictory. We develop a model for the thermal conductivity of a nanofluid, which provides much higher predictions than the standard Maxwell model and a better match to data.

Keywords: carbon nanotubes, enhanced flow, nanoparticle melting, thermal conductivity, nanofluid

1 INTRODUCTION

Advances in nanotechnology are primarily driven by experimental research, whilst in other disciplines many breakthroughs come through theory or simulation. This may be partially explained by the fact that standard theories, based on the continuum assumption, often fail to reproduce experimental observations of nano-phenomena. However, there are a number of studies indicating that continuum theory may be applied down to a few nanometres. For example Guisbiers *et al* [1] suggest continuum theory may be applied to the melting of nanoparticles with radii greater than 2nm. Travis *et al* [2] compare molecular dynamics with results from the Navier-Stokes equation to show that continuum theory holds for water flow down to around 3nm. In this paper we will apply continuum theory to problems in fluid and heat flow and demonstrate how seemingly anomalous behaviour may be explained without resorting to molecular dynamics or empirically based adjustments.

2 ENHANCED FLOW IN CNTs

The classical model for flow in a circular cylindrical pipe is described by the Hagen-Poiseuille equation which leads to an expression for the fluid flux:

$$Q_{HP} = -\pi R^4 p_z/(8\mu)\,, \tag{1}$$

where p_z is the pressure gradient along the pipe, R is the radius and μ the fluid viscosity. In CNTs it is well documented that the flux is significantly higher than this value. Papers in *Nature* and *Science* reported increases by orders of magnitude, although recent work provides more conservative estimates: Whitby *et al* [5] quote a maximum increase by a factor of 45.

A popular approach to explain this enhancement is to introduce a slip-length into the mathematical model, that is, the no-slip boundary condition $u(R) = 0$ is replaced by $u(R) = -L_s \frac{\partial u(R)}{\partial r}$ where L_s is the slip-length and u the velocity. This leads to a flux expression

$$Q_{slip} = Q_{HP}\,(1 + 4L_s/R)\,. \tag{2}$$

Hence any magnitude of enhancement can be accounted for by using an appropriate value for L_s. Comparison of theory with experiments on the microscale lead to sensible values of the slip length, which are much smaller than the channel dimension. Yet, when dealing with nanochannels the slip lengths are typically on the order of microns. This has led to scepticism concerning the validity of the slip modified Hagen-Poiseuille model.

An alternative explanation to the slip-length is based on the fact that CNTs are hydrophobic. The strength of attraction between water molecules is greater than the attraction between the hydrophobic solid and the water. It has been postulated that hydrophobicity may result in gas gaps, depletion layers or the formation of vapour: all descriptions result in a region of low viscosity close to the wall and experimentally this may be interpreted as 'apparent' slippage. Poynor *et al* [6] state that their synchrotron x-ray data unambiguously demonstrates a depletion layer is formed when water meets a hydrophobic surface. Depletion layers have also been predicted via molecular dynamics (MD) simulations.

Myers [7] proposes a mathematical solution based on the presence of a depletion layer. Standard fluid equations are employed but using two distinct regions: a bulk flow region occupying the centre of the channel

and a depleted region with low viscosity near the walls. This leads to a flux defined by

$$Q_\mu = Q_{HP}(\alpha^4/R^4)\left(1+(\mu_1/\mu_2)\left((R^4/\alpha^4)-1\right)\right), \qquad (3)$$

where μ_1, μ_2 represent the bulk and depletion layer viscosities respectively, $\mu_1 \gg \mu_2$ and α is the radius of the bulk region (for CNTs experiments indicate a depletion layer thickness $\delta = 0.7$nm, hence $\alpha = R - 0.7$nm). The flow enhancement is defined as the ratio $\epsilon_\mu = Q_\mu/Q_{HP}$. Taking data from [5] it turns out that $\mu_2 \approx 0.018\mu_1$. The viscosity of air and oxygen are approximately 0.02 that of water.

With gas flow there is a theory to account for apparent slip, with a slip-length on the order of the gas mean free path however no such theory has been found for fluids. Comparison of the above flux expressions with slip and a depletion layer leads to an expression for an effective slip-length for a fluid

$$L_s = \delta\left(\frac{\mu_1}{\mu_2}-1\right)\left[1-\frac{3}{2}\frac{\delta}{R}+\left(\frac{\delta}{R}\right)^2-\frac{1}{4}\left(\frac{\delta}{R}\right)^3\right]. \qquad (4)$$

Further, noting that $\mu_1/\mu_2 \gg 1$, we can identify three distinct regimes:
1. For sufficiently wide tubes, such that $\delta/R \ll \mu_2/\mu_1$, then $\epsilon_\mu \approx 1$. There is no noticeable flow enhancement and the no-slip boundary condition will be sufficient, $L_s \approx 0$. This should hold approximately for $R > 3\mu$m.
2. For moderate tubes, such that $(\delta/R)(\mu_1/\mu_2)$ is order 1 but $\delta/R \ll 1$ then only the leading order term of L_s applies and

$$\epsilon_\mu \approx 1 + (4\delta/R)\,(\mu_1/\mu_2 - 1)\,. \qquad (5)$$

This holds approximately for $R \in [21\text{nm}, 3\mu\text{m}]$.
3. For very small tubes where δ/R is order 1 then the full expression for ϵ_μ is required.

The above model and conclusions fit well, both quantitatively and qualitatively, with experimental evidence. For example, numerous papers report constant slip-lengths of 20-40nm for R ranging from 'some nanometers up to several hundreds of nanometers'[3]. Thomas *et al* [4] suggest L_s varies with R for $R \in [1.6, 5]$nm and show $\epsilon \approx 32$ when $R = 3.5$nm. The above model predicts $\epsilon \approx 33.2$ for this R value. It also predicts a maximum enhancement of around 50 which compares well with the maximum value of 45 observed by Whitby *et al* [5].

3 NANOPARTICLE MELTING

Nanoparticles are often employed in harsh environments where they are prone to melting. In fact many applications require the particles to melt, after serving their primary purpose, and so pass through the system as disperse molecules. Hence it is important to understand the thermal response of a nanoparticle and its likely phase change behaviour.

It is well-documented that the phase change temperature decreases as the material dimensions decrease. With gold experiments have shown decrease of around 500K below the bulk melt temperature for particles with radius slightly greater than 1nm [9]. MD simulations have shown even greater decreases. A study of antibiotic and antianginal drugs shows a melting point depression of around 30K (a 10% decrease from the bulk value)[10].

If the density and specific heat remain approximately constant in each phase the melt temperature may be estimated from the following generalised Gibbs-Thomson relation

$$L_m\left(\frac{T_m}{T_m^*}-1\right)+\Delta c\left[T_m\ln\left(\frac{T_m}{T_m^*}\right)+T_m^*-T_m\right] = -\frac{2\sigma_{sl}\kappa}{\rho_s} \qquad (6)$$

where L_m is the latent heat, T_m is the temperature at which the phase change occurs, T_m^* the bulk phase change temperature, $\Delta c = c_l - c_s$ the change in specific heat from liquid to solid, σ the surface tension and κ the mean curvature. Figure 1 compares results for the generalised Gibbs-Thomson relation against experiment for gold nanoparticles between 2 and 12 nm, see [8]. In

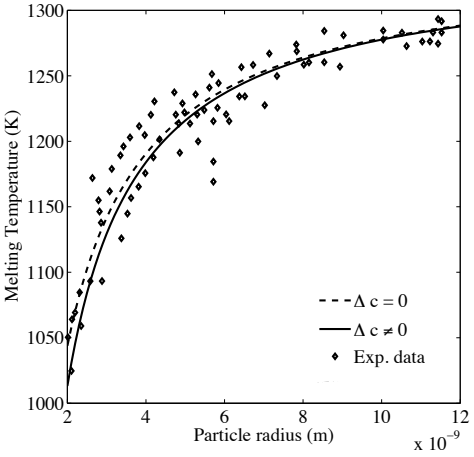

Figure 1: Variation of the melt temperature of gold nanoparticles

Font *et al* [8] a mathematical model for the melting of a spherically symmetric nanoparticle is analysed. The model is based on standard phase change theory, specifying heat equations in the solid and liquid phases while the position of the melt front $R(t)$ is determined from an energy balance. The melt temperature is specified by the above Gibbs-Thomson relation. This system is difficult to solve analytically consequently the equations are non-dimensionalised to identify dominant terms. The energy balance is then

$$\left[1+\frac{(1-c)}{\beta}T_m\right]\frac{dR}{dt} = -\left.\frac{\partial T}{\partial r}\right|_{r=R} - k\frac{\partial\theta}{\partial r}. \qquad (7)$$

where $\beta = L_m/(c_l\Delta T)$, k is the conductivity ratio, c the specific heat ratio and T, θ represent the temperature in the liquid and solid respectively.

Noting that β is typically large (for gold heated 10K above the bulk melt temperature $\beta \approx 40$) permits the use of a standard perturbation technique to simplify the problem. This technique reduces the system to a single ordinary differential equation for R coupled to the Gibbs-Thomson relation to determine T_m:

$$\frac{dR}{dt} = \frac{(T_m - 1)}{R(1-R)} \left[\beta + (1-c)T_m - \frac{c_1}{3}\frac{(1-R)^2}{R} - 2kc_2R \right]^{-1} \tag{8}$$

where c_i are known functions of R, T_m. Obviously a single ordinary differential equation is much simpler to solve than a pair of partial differential equations specified over an unknown region. Further, this model clearly shows that as $R \to 0$ the velocity $R_t \to \infty$, thus explaining the rapid disappearance of nanoparticles in the final stages of melting In Figure 2 we show the evolution of the melt front, $R(t)$, with time. The dashed lines are the approximate solution, the solid lines come from a numerical solution of the full system. The three sets of curves represent three solution forms, the curves labelled (i) represent the model using the generalised Gibbs-Thomson relation, curves (ii) take $c_s = c_l$ in Gibbs-Thomson but not the energy balance and curves (iii) are the classical model where $c_s = c_l$ and $T_m = T_m^*$. It is clear that the classical model will overpredict the melt time by a significant amount (usually at least by an order of magnitude). Curves (ii) and (iii) demonstrate how, as the solid radius decreases, the gradient of the curve increases and tends to infinity. This is not explained by the classical theory. Figure 3 shows the temperature profile within the liquid and solid regions as the particle melts. The dotted line indicates how the melt temperature decreases with time.

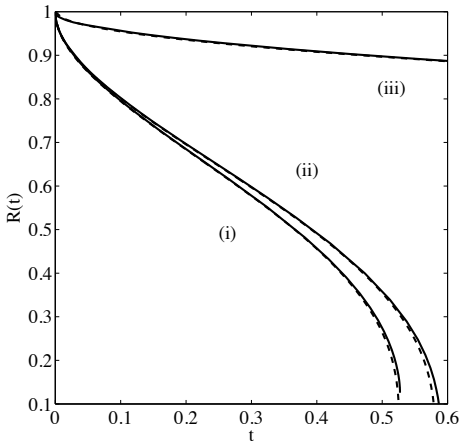

Figure 2: Typical result for non-dimensional position of melt front $R(t)$ (to convert to dimensional form multiply R by the original particle radius of 10nm and t by the time-scale 2.7ps)

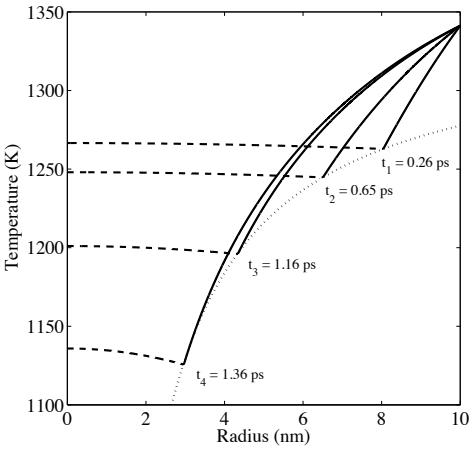

Figure 3: Temperature profiles within a melting nanoparticle

4 THERMAL CONDUCTIVITY OF NANOFLUIDS

There exists a vast literature on the enhanced thermal properties of nanofluids when compared to their base fluids. The often remarkable enhancement then suggests nanofluids as the solution for heat removal in many modern electronic devices. However there are discrepancies and much debate over experimental findings and so far no satisfactory mathematical model has been proposed to describe the thermal response of a nanofluid.

The classical analysis of heat conduction for solid-in-liquid suspensions is that of Maxwell, based on effective medium theory. This leads to an expression for the effective thermal conductivity

$$\frac{k_e}{k_l} = \left[\frac{2k_l + k_p + 2\phi(k_p - k_l)}{2k_l + k_p - \phi(k_p - k_l)} \right], \tag{9}$$

where k_e, k_p, k_l represent the effective, particle and liquid thermal conductivity and ϕ is the particle volume fraction. There are obvious problems with the Maxwell model. Firstly, it is based on analysing the heat flow in the material surrounding an equivalent nanofluid and the heat flow around a particle, as opposed to analysing the actual nanofluid or particle behaviour. The analysis is carried out over an infinite region. Hence the result can only be applied to a highly disperse fluid where the particles are so far apart that an energy change in one has a negligible effect on any other particle. This approach will clearly lead to problems as the particle concentration increases. Further, the Maxwell model is based on a steady-state solution but in general one would wish to analyse how a nanofluid responds in a time-dependent situation.

Keblinski *et al* [11] compared the data from various groups working with nanofluids and found that

for most of the data $k_e \approx (1 + C_k\phi)k_l$ with $C_k \approx 5$ whilst the linearised Maxwell model predicts $C_k \approx 3$. In an attempt to improve the fit between theory and experiment various researchers have extended or modified Maxwell's model to account for nanolayers, particle clustering, nanoconvection and Brownian motion. In each case the introduction of new effects and new parameters permits better agreement with certain experiments.

Myers *et al* [12] investigate a time-dependent model for heat flow through a particle and finite volume of liquid. The exact solution of the system is complicated, involving infinite series of Bessel's functions. This makes it very difficult to identify the contribution of the various problem parameters. As in the previous example, the system is non-dimensionalised. This new system indicates an obvious simplification based on the fact that the nanoparticle has a much higher thermal diffusivity than the fluid (for Al_2O_3 in water the particle/fluid diffusivity ratio is approximately 60, for CuO in ethylene glycol it is 1200). An accurate approximate solution technique, known as the Heat Balance Integral Method, is also employed. This permits simple polynomial approximations to the temperature in the fluid and particle and, more importantly, clearly shows the effect of the problem parameters. A similar analysis is carried out on an equivalent fluid system (i.e. a fluid that will imitate a fluid-particle system behaviour). By equating the decay rates of the two models an expression for the thermal conductivity of the equivalent fluid is determined

$$\frac{k_e}{k_l} = \frac{\left[(1-\phi) + \phi\frac{\rho_p c_p}{\rho_l c_l}\right](n-1)}{(1-\phi^{1/3})^2\left[(1+\phi^{1/3})(n+1)-2\right]} \qquad (10)$$

According to this formula, the equivalent particle conductivity is independent of the particle conductivity (this has been observed experimentally). The particle material enters through the density and specific heat $(\rho c)_p$, but since the ratio $\rho_p c_p/(\rho_l c_l)$ is order 1 and ϕ is small this is a weak dependence. Hence the effective conductivity is primarily a function of the liquid conductivity k_l and volume fraction ϕ. The true test of a theory comes through comparison with experiment. In Figures 4, 5 we compare the present prediction for k_e with that of Maxwell and a number of data sets taken from the literature. As expected, there is quite a spread in the data and so we cannot hope to match all points. Figure 4 shows results for an Al_2O_3-water nanofluid. The prediction of the current theory, given by equation (10), is shown as the solid line, the Maxwell result of equation (9) is the dashed line. For very low volume fractions the Maxwell curve lies above the prediction of (10) and captures the data better, but for $\phi > 0.008$ (i.e. a volume fraction around 0.8% the present model rapidly increases above Maxwell and, more importantly, passes between a large amount of the experimental data. Figure 5 shows results for a Cu-ethylene glycol nanofluid. In both figures it is clear that the present model provides a much better approximation to the majority of experimental data when compared to the basic Maxwell model for volume fractions approximately greater than 1%.

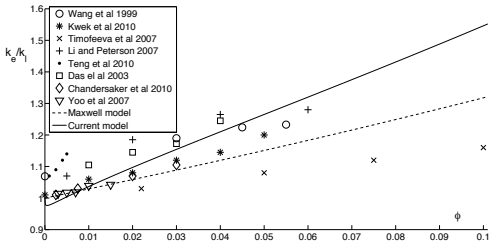

Figure 4: Conductivity ratio k_e/k_l for Al_2O_3-water nanofluid with $k_l = 0.58$W/mK: equation (10) (solid line); Maxwell model equation (9) (dashed line) and experimental data.

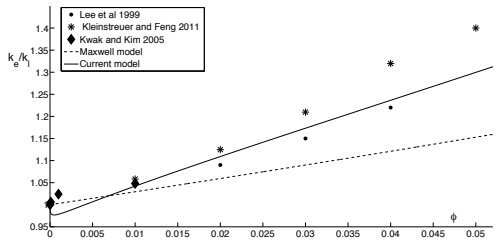

Figure 5: Conductivity ratio k_e/k_l for CuO-ethylene glycol nanofluid with $k_l = 0.258$W/mK: equation (10) (solid line); Maxwell model equation (9) (dashed line) and experimental data.

REFERENCES

[1] G. Guisbiers *et al.* J. Phys Chem C, 112, 4097-4103, 2008.

[2] K.P. Travis *et al.* Phys Rev E 55(4), 4288-4295, 1997.

[3] C. Cottin-Bizonne *et al.* PRL 94, 056102, 2005.

[4] J.A. Thomas *et al.* Int. J. Therm. Sci. 49, 281289, 2010.

[5] M. Whitby *et al.* Nanoletters 8(9), 2632-2637, 2008.

[6] A. Poynor PRL 97, 266101, 2006.

[7] T.G. Myers Microfluid. Nanofluid. 2010 DOI: 10.1007/s10404-010-0752-7.

[8] F. Font *et al.* Sumitted to J. Nanopar Res. 2013.

[9] Ph. Buffat *et al.* Phys Rev A 13(6), 2287-2298, 1976.

[10] X. Liu *et al* Mat Chem Phys 103, 1-4, 2007.

[11] P. Keblinski *et al.* J Nanopart Res, 10:10891097, 2008.

[12] T.G. Myers *et al.* Sumitted to J. Nanopar Res. 2013.